

Phase Segregation in Silicon Carbide–Carbon Solid Solutions from XRD and NMR Studies

Oleksandr O. Mykhaylyk,[†] Yaroslav Z. Khimyak, and J. Paul Attfield*

Department of Chemistry, University of Cambridge, Lensfield Road,
Cambridge CB2 1EW, United Kingdom

Mykola P. Gadzira

Institute for Problems of Materials Science, NAS of Ukraine, 3 Krzhyzhanivskogo str.,
Kyiv 03142, Ukraine

Received September 24, 2001. Revised Manuscript Received December 5, 2001

SiC–C solid solution powders have been analyzed by X-ray diffraction (XRD) and magic-angle spinning nuclear magnetic resonance (MAS NMR). The XRD data reveal a previously unreported phase separation of the as-synthesized material into two cubic silicon carbide phases characterized by slightly different lattice parameters [4.35287(9) and 4.35841(6) Å]. The ²⁹Si MAS NMR spectra of the powders after different heat treatments (annealing in a vacuum and high-pressure sintering) show that the small excess of carbon (<1 at %) in the β-SiC crystal structure has a large influence on the ²⁹Si chemical shift resulting in a displacement of the ²⁹Si MAS NMR peak from –18.5 ppm to lower field. At least five nonequivalent silicon sites have been detected in Si_{1–x}C_{1+x}: the solid solution formed by high-pressure sintering (4 GPa, 1800 °C) of the as-synthesized SiC–C powder. These sites are assigned to point (carbon antisite) defects in the cubic silicon carbide structure.

Introduction

Silicon carbide (SiC) is important as an ultrahard ceramic material. It is known to exist in various polytypic forms, of which the common forms are 3C, 4H, 6H, and 15R.¹ All forms of silicon carbide are based on the diamond-like structure, with alternating, tetrahedrally bonded, silicon and carbon atoms. The cubic polytype, 3C, has a stacking sequence of diamond-like planes of Si and C with only one type of crystallographic site for Si and C atoms. All the other SiC polytypes are formed by other stacking sequences of Si and C layers and have trigonal, hexagonal, or rhombohedral symmetries. It is well established that the arrangement of the layer units in the silicon carbide polytypes can include stacking faults.^{2,3} Recently, it was shown that in addition to stacking faults, certain synthesis processes can produce diamond-like C layers in the cubic silicon carbide (β-SiC) crystal structure forming a SiC–C solid solution.⁴ Thus, the superstoichiometric carbon atoms are located in the silicon carbide crystal structure as planar defects along {111}. These defects

reduce the lattice parameter and produce strain anisotropy in the β-SiC crystal structure.⁵ It was revealed that a diffusion of the superstoichiometric carbon atoms during high-pressure and high-temperature sintering (4 GPa, 1800 °C) breaks down the planar defects producing an ideal solid solution of carbon in the silicon sublattice of the β-SiC crystal structure. The lattice parameter of this sintered sample has been used to estimate the composition through Vegard's law as Si_{1–x}C_{1+x} with $x = 0.007$.⁴ The presence of superstoichiometric carbon in the silicon carbide crystal structure changes the local atomic environment and can produce electronically nonequivalent sites.

During the last two decades, it has been shown that solid-state magic-angle spinning nuclear magnetic resonance (MAS NMR) spectroscopy is ideally suited to determine the number of crystallographically nonequivalent sites in SiC polytypes.^{6–8} The ²⁹Si and ¹³C chemical shifts demonstrate high sensitivity to the environments of these atoms beyond their nearest neighbors. One can therefore expect MAS NMR spectroscopy to be sensitive to the number and types of local environments in the SiC–C solid solutions and provide supplementary information to elucidate the location of the superstoichiometric carbon atoms in the structure. Thus, the application of X-ray diffraction (XRD) measurements to study long-range structural order along

* To whom correspondence should be addressed. E-mail: jpa14@cam.ac.uk.

[†] Permanent address: Institute for Problems of Materials Science, NAS of Ukraine, 3 Krzhyzhanivskogo str., Kyiv 03142, Ukraine.

(1) Verma, A. R.; Krishna, P. *Polymorphism and Polytypism in Crystals*; Wiley: New York, 1966; *Gmelin Handbook of Inorganic Chemistry*, 8th ed.; Springer-Verlag: Berlin/Heidelberg/New York; Suppl. Vol. B2, Si–Silicon, "Properties of Crystalline Silicon Carbide", 1984; Suppl. Vol. B3, Si–Silicon, "System Si–C", 1986.

(2) Jagodzinski, H. *Acta Crystallogr.* **1954**, *7*, 300.

(3) Pandey, D.; Lele, S.; Krishna, P. *Proc. R. Soc. London* **1980**, *A369*, 435.

(4) Mykhaylyk, O. O.; Gadzira, M. P. *Acta Crystallogr.* **1999**, *B55*, 297.

(5) Mykhaylyk, O. O.; Gadzira, M. P. *J. Mater. Chem.* **2001**, *11*, 217.

(6) Hartman, J. S.; Richardson, M. F.; Sherriff, B. L.; Winsborrow, B. G. *J. Am. Chem. Soc.* **1987**, *109*, 6059.

(7) Guth, J. R.; Petuskey, W. T. *J. Phys. Chem.* **1987**, *91*, 5361.

(8) Dybowski, C.; Gaffney, E. J.; Sayir, A.; Rabinowitz, M. J. *Colloids Surf.* **1996**, *A118*, 171.

with MAS NMR spectroscopy can provide detailed insights about the structure of SiC–C solid solutions, as described below. An excellent example of this approach is an analysis of the stacking fault distribution in β -SiC.⁹

Experimental Section

Sample Preparation and Characterization. The SiC–C solid solution powder was synthesized by self-propagating high-temperature synthesis (the ignition temperature was in the range of 1200–1300 °C) in an argon atmosphere from a mixture of fine elemental silicon powder and thermally exfoliated graphite (TEG). The particle size of the synthesized powder is less than 1 μm . The details of the preparation of the powder are described elsewhere.¹⁰ The XRD pattern showed the presence of stacking faults in the cubic SiC–C crystal structure,⁴ and together with the main phase, the synthesized powder included small quantities of Si_3N_4 and $\text{Si}_2\text{N}_2\text{O}$. There were no significant amount of amorphous components identified by the XRD experiment. Subsequently, the as-synthesized SiC–C powder was annealed in a vacuum at different temperatures in the range of 1400–1900 °C and sintered under pressures in the range of 4–8 GPa and temperatures of 1400 and 1800 °C. The mechanical properties of these and other samples are reported elsewhere.⁵ To carry out the NMR measurements, the sintered samples were crushed in an agate mortar. These samples were tested by XRD before and after crushing, and no significant change in the lattice parameter and peak broadening was observed.

Instrumental and Measuring Techniques. Initial powder XRD data were collected on a DRON–UM1 powder diffractometer [graphite (002) monochromator, Cu $K\alpha$ radiation] operated in a reflection scan mode. To obtain higher resolution diffraction measurements, a STOE STADI P powder diffractometer [position sensitive detector, curved germanium (111) monochromator, Cu $K\alpha_1$ radiation, $\lambda = 1.5405981$ Å] operated in transmission scan mode was used. The upper 2θ limit of 130° enabled the diffraction pattern of cubic silicon carbide to be recorded up to the 224 reflection. Throughout the experiments, the ambient temperature was maintained at 21 ± 0.5 °C. The systematic errors of the measurements such as the zero shift of diffractometer ($< \pm 0.003^\circ$) and displacement of specimens from the goniometer axis ($< \pm 0.02$ mm) were determined at the beginning and at the end of each pattern. The diffraction patterns were fitted by a full profile Rietveld method using the Fullprof software package.¹¹ Individual peaks were also fitted with the CSD software package (version 4.11)¹² using a pseudo-Voigt function. This package was also applied for least-squares refinement of lattice parameters. The shifts of diffraction lines caused by the displacement of the specimens from the goniometer axis were taken into account in the calculations. The lattice parameter values were not corrected for refraction.

The alignment of the STOE diffractometer was tested by a silicon standard (SRM640b) and β -SiC (the fine powder was synthesized¹³ by the reaction of SiO_2 and C and annealed at 1800 °C to obtain a stacking-fault-free structure of cubic silicon carbide). The lattice parameters determined for these materials [5.43093(5) and 4.35883(7) Å, respectively] were in a good agreement with literature data [5.430969(39)¹⁴ and 4.3589(1) Å,¹⁵ respectively]. The instrumental resolution of the STOE

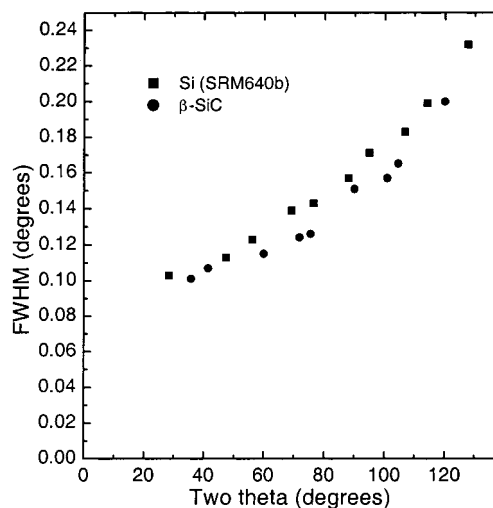


Figure 1. Instrumental resolution of STOE STADI P diffractometer. The FWHM vs 2θ for diffraction lines of silicon standard (SRM640b) and β -SiC powder.

diffractometer estimated by the full widths at half-maximum (FWHM) of the silicon standard and β -SiC peaks was ca. 0.10° at lower 2θ diffraction angles and ca. 0.20° at higher 2θ diffraction angles (Figure 1).

Solid-state ^{29}Si and ^{13}C MAS NMR spectra were recorded at 9.4 T (79.44 MHz for ^{29}Si and 100.56 MHz for ^{13}C) using a Chemagnetics CMX-400 spectrometer with a 4 mm diameter zirconia rotor spun in nitrogen at 8.0 kHz. All MAS NMR spectra presented in the paper were obtained by using $\pi/4$ pulses of 2.0 μs duration with a recycle delay of 600 s. At least 68 repeated scans were acquired. Chemical shifts are quoted in ppm from external tetramethylsilane. A deconvolution of the NMR spectra was carried out using the Spinsight 4.1 software package. Spin–lattice relaxation times (T_1) were determined using the standard saturation-recovery method. The curve-fitting analysis of variable delay time data was used to calculate the T_1 . The above β -SiC powder was used as the β -SiC standard for the MAS NMR measurements.

Electron spin resonance (ESR) spectra were recorded on a Bruker ER 200 D EPR spectrometer with an X-band cavity and a microwave frequency of 8.97 GHz. This instrument is sensitive to ~ 1 ppm of unpaired spins.

Results and Discussion

XRD Analysis. On the basis of diffraction peak broadening (Williamson–Hall plots) and an analysis of the behavior of the lattice parameter following different treatments at high temperatures in a vacuum or under high pressures, a structural model of the solid solution SiC–C was previously suggested.⁴ In this model, superstoichiometric carbon atoms are located in diamond-like layers and form planar defects along $\{111\}$ in cubic SiC–C. Such defects lead to a decrease of the lattice parameter of silicon carbide, broadening of the diffraction peaks, and strain anisotropy of the crystal structure.^{4,5} The higher resolution of XRD in the present investigation reveals a previously unobserved splitting of the diffraction peaks for the as-synthesized powder, which is most clearly observed at high 2θ angles (Figure 2). The absence of an hkl dependence of the splitting eliminates the possibility of a slight hexagonal or other lattice distortion. The splittings are consistent with a

(9) Tateyama, H.; Noma, H.; Adachi, Y.; Komatsu, M. *Chem. Mater.* **1997**, *9*, 766.

(10) Gadzyra, N. F.; Gnesin, G. G.; Andreev, A. V.; Kravets, V. G.; Kasyanenko, A. A. *Inorg. Mater.* **1996**, *32*, 721.

(11) Rodriguez-Carvajal, J. Fullprof Program, Version 3.5d. Laboratoire Leon Brillouin, France, 1998.

(12) Akselrud, L. G.; Gryn, Yu. N.; Zavalii, P. Y.; Pecharskii, V. K.; Fundamentalskii, V. S. *Twelfth European Crystallographic Meeting*, Moscow, USSR, August 20–29, 1989; Collected Abstracts; Oldenburg: München, 1990; Vol. 3, p 155.

(13) Khaenko, B. V.; Prilutskii, E. V.; Mikhailik, A. A.; Karpets, M. V.; Krainikov, A. V. *Inorg. Mater.* **1995**, *31*, 304.

(14) Yoder-Short, D. *J. Appl. Crystallogr.* **1993**, *26*, 272.

(15) Powder Diffraction File No. 29-1129; $a = 4.3589(1)$ Å; the wavelength for Cu $K\alpha$ radiation was taken to be 1.54178 Å.

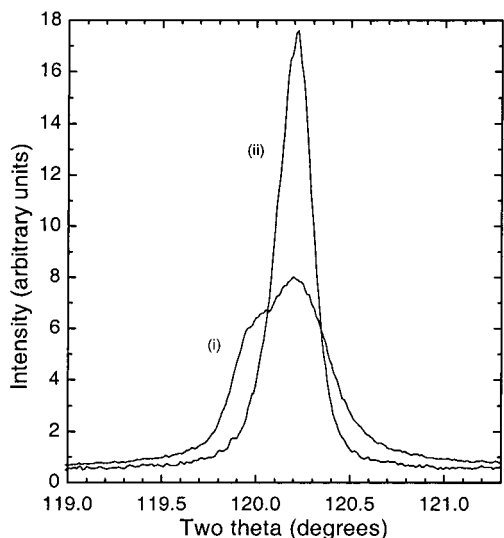


Figure 2. XRD pattern (STOE diffractometer, Cu $K\alpha_1$ radiation) of the $224_{\beta\text{-SiC}}$ reflection for silicon carbide: (i) as-synthesized powder and (ii) crushed sample after high-pressure sintering at 4 GPa and 1800 °C.

two-phase behavior, showing that the concentration of the superstoichiometric carbon layers in the SiC–C structure is not uniform, and the previous model for the as-synthesized SiC–C materials⁴ requires modification.

Rietveld fitting of two cubic silicon carbide phases (space group $F\bar{4}3m$) to the XRD data was unsuccessful because of the similarity in the cell parameters of the two phases. However, an individual deconvolution of each of the XRD peaks enabled the two contributions to be distinguished and the estimated peak positions correspond to two face-centered cubic crystal structures, SiC–C and $\beta\text{-SiC}$, with lattice parameters of 4.35287(9) and 4.35841(6) Å, respectively. The latter is slightly lower than the value of 4.3589(1) Å for standard $\beta\text{-SiC}$.¹⁵ The deconvoluted relative intensities of the reflections for the two phases appear to be different from the calculated intensities for cubic silicon carbide,¹⁶ but a higher resolution diffraction experiment using synchrotron radiation will be needed to characterize the two structures more accurately.

The sintering of the as-synthesized powder at a high pressure (4–8 GPa) and temperature (1800 °C) leads to the disappearance of the splitting in the silicon carbide diffraction pattern, and sharp peaks from a single cubic phase with a lattice parameter of 4.35286(4) Å were observed after sintering at the lowest pressure of 4 GPa (Figure 2). If a mixture of two individual phases of silicon carbide ($\beta\text{-SiC}$ and SiC–C) is assumed to occur in the as-synthesized powder, then the $\beta\text{-SiC}$ lattice parameter should decrease after such treatments. However, no lattice parameter decrease is observed after heat treatment of stoichiometric $\beta\text{-SiC}$ under such pressures¹⁷ and the model discussed below shows that a mixture of the two individual phases is not a good description of the structural transformation on sintering.

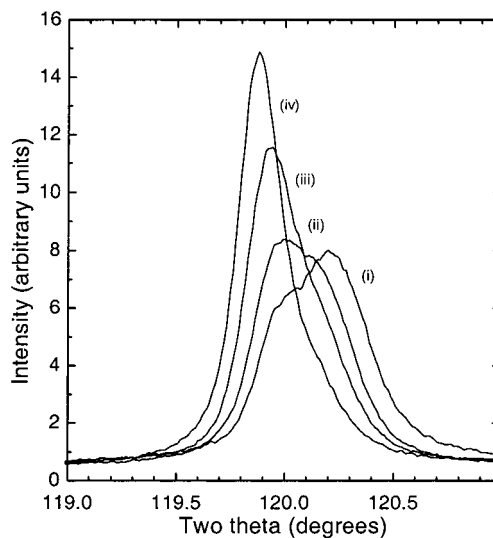


Figure 3. XRD pattern (STOE diffractometer, Cu $K\alpha_1$ radiation) of the $224_{\beta\text{-SiC}}$ reflection for silicon carbide powder: (i) as-synthesized, (ii) annealed at 1600 °C, (iii) annealed at 1700 °C, and (iv) annealed at 1900 °C.

A small correction to the previous structural model⁴ of the SiC–C solid solution is needed to satisfy the results of the diffraction experiments. In this model, planar diamond-like carbon defect layers exist in silicon carbide. If these tend to aggregate in some regions of the SiC, then domains of $\beta\text{-SiC}$ and SiC–C will exist in the crystallites, and if they are sufficiently large, a splitting of the diffraction peaks will be observed. Diffusion at high pressures and a temperature of > 1800 °C breaks down the superstoichiometric carbon layers in the SiC–C crystal structure and establishes a uniform concentration of the excess of carbon atoms in all parts of the crystallites. Thus, the thermal diffusion at 4 GPa and 1800 °C equalizes the composition of the $\beta\text{-SiC}$ and SiC–C domains and an ideal, homogeneous, single-phase solid solution ($\text{Si}_{1-x}\text{C}_{1+x}$) is produced. The diffusion of superstoichiometric carbon atoms at the (4 GPa, 1800 °C) sintering changes the microstructure from planar long-range defects in the phase-segregated, as-synthesized SiC–C solid solution to point defects (C_{Si} antisites) in the ideal solid solution, so that the average lattice parameter is not conserved during the process. Sintering the as-synthesized powder at a lower temperature of 1400 °C (when this diffusion process is not active) does not change the fine structure of the XRD pattern, and only a broadening of the peaks created by an increase of the dislocation density was observed.⁵

After the annealing of the as-synthesized powder in a vacuum, the splitting of the silicon carbide diffraction peaks remains at all applied temperatures. However, the intensity of the higher angle component of the peaks corresponding to the SiC–C solid solution is reduced as the annealing temperature increases (Figure 3) showing that the fraction of carbon-rich SiC–C decreases. As a result, the diffraction pattern of the powder heated at 1900 °C is almost identical to that of standard $\beta\text{-SiC}$. The main cause of the destruction of the SiC–C is a breakdown of the C–C bonds in the diamond-like planes at temperatures higher than 1400 °C in a vacuum.^{4,18} In addition, a slight shift of the peaks to lower angles is observed in the diffraction patterns with increasing temperature (Figure 3). The estimation

(16) $\beta\text{-SiC}$ and SiC–C have similar relative diffraction intensities, see: Gadzira, M.; Gnesin, G.; Mykhaylyk, O.; Andreyev, O. *Diamond Relat. Mater.* **1998**, *7*, 1466.

(17) Palosz, B.; Stelmakh, S.; Gierlotka, S.; Aloszyna, M.; Pielaszek, R.; Zinn, P.; Peun, T.; Bismayer, U.; Keil, D. G. *Mater. Sci. Forum* **1998**, *278*, 612.

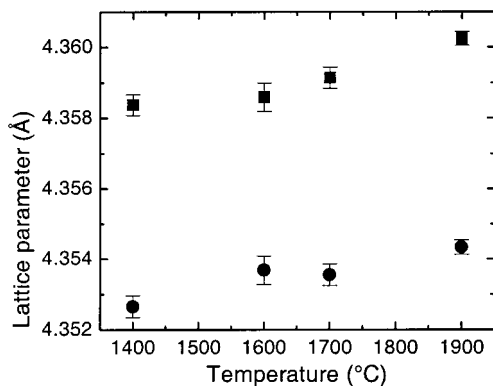


Figure 4. Dependence of the lattice parameter of the β -SiC (■) and the SiC–C (●) regions on the annealing temperature of the synthesized powder.

of the lattice parameters based on the deconvolution of the most highly resolved, 224, reflection shows that the parameter increases slightly for both the β -SiC and SiC–C regions in the crystallites (Figure 4). This suggests that the two different types of silicon carbide in a crystallite have a mutual influence on each other, presumably through epitaxial interfaces, and a high fraction of SiC–C domains leads to a slight decrease of the lattice parameter for the rest of the silicon carbide (β -SiC). The growth of the cubic silicon carbide fraction at high annealing temperatures (Figure 3) leads to a gradual increase of the β -SiC lattice parameter until the standard value is reached (Figure 4).

NMR Analysis. The excess carbon atoms in SiC–C could change the local bonding of the atoms and create dangling bonds as in amorphous $\text{Si}_{1-x}\text{C}_x$.¹⁹ However, no ESR signal was detected for the as-synthesized powder showing that SiC–C is diamagnetic and has a negligible concentration of dangling bonds or incorporated impurities such as nitrogen²⁰ with unpaired electrons. The absence of paramagnetic centers enabled MAS NMR spectroscopy to be applied to these silicon carbide samples. Attempts to record ¹³C NMR spectra were unsuccessful, as in other NMR studies^{6,7} of cubic silicon carbide. This is probably due to the extremely long spin–lattice relaxation time. Hence, only ²⁹Si MAS NMR results were used to analyze the SiC–C materials.

The ²⁹Si MAS NMR spectrum of the as-synthesized powder shows a sharp peak at -18.5 ppm together with a downfield shoulder [Figure 5, (i)]. The position of the peak is in good agreement with ²⁹Si MAS NMR data for standard β -SiC obtained both in the present research [Figure 4, (iv)] and in other investigations.^{6,7,21} Stacking faults,⁹ which were identified by previous XRD experiments,⁴ create several types of inequivalent sites for Si which generate additional shoulders on both sides of the main ²⁹Si NMR peak, so the absence of an upfield shoulder in the ²⁹Si NMR spectrum indicates that the

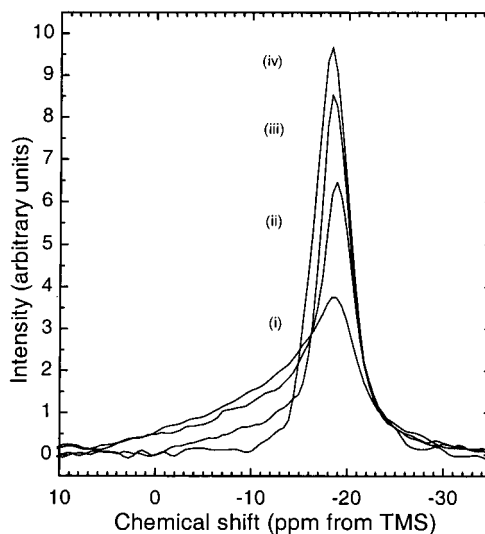


Figure 5. ²⁹Si MAS NMR spectra of silicon carbide powders: (i) as-synthesized, (ii) annealed at 1600 °C, (iii) annealed at 1700 °C, and (iv) standard β -SiC.

fine structure is not caused by these faults. Instead, structural defects due to the excess of carbon in the silicon carbide are identified as the cause of the downfield shoulder in the ²⁹Si NMR spectrum of the as-synthesized powder.

If the above domain model of the as-synthesized SiC–C solid solution is followed, the sharp peak in the ²⁹Si NMR spectra at ca. -18.5 ppm can be assigned to sites in the β -SiC regions and the downfield shoulder represents silicon atoms located in the SiC–C domains. This assignment is supported by basic solid-state ²⁹Si MAS NMR results. The chemical shift for elemental silicon in the diamond-like crystal structure is -80.6 ppm,⁶ and the substitution of half the silicon atoms by carbon atoms to give the cubic silicon carbide structure shifts the position of the ²⁹Si MAS NMR peak to ca. -19 ppm.^{6,7} It is reasonable to suggest that a further slight increase of the amount of carbon in the silicon carbide structure to create the SiC–C solid solution will shift the silicon NMR peak to lower fields. The broad shoulder is thus a superposition of several overlapping ²⁹Si MAS NMR resonances corresponding to different silicon environments in the carbon-rich SiC–C regions of the crystallites.

The spin–lattice relaxation times estimated from ²⁹Si saturation-recovery spectra of the as-synthesized powder showed a significant difference between the broad and sharp components of the spectrum. As a result, the position of the center of gravity of the whole signal of superimposed silicon peak shifts upfield with the increased recovery time. The plot of the intensity of the NMR signal at -18.5 ppm vs recovery delay τ shows an exponential-like dependence (Figure 6) with the best fit obtained using a double exponential function of the form

$$y = M_0^{\text{SiC}}(1 - \exp[-\tau/T_1^{\text{SiC}}]) + M_0^{\text{SiC-C}}(1 - \exp[-\tau/T_1^{\text{SiC-C}}])$$

from which T_1^{SiC} and $T_1^{\text{SiC-C}}$, the spin–lattice relaxation times of the two different types of silicon sites, can be derived (M_0^{SiC} and $M_0^{\text{SiC-C}}$ are the corresponding am-

(18) Evans, T.; James, R. A. *Proc. R. Soc. London* **1964**, A277, 260.

(19) (a) Shimizu, T.; Kumeda, M.; Kiriya, Y. *Solid State Commun.* **1981**, 37, 699. (b) Ishii, N.; Kumeda, M.; Shimizu, T. *Solid State Commun.* **1982**, 41, 143.

(20) (a) GreulichWeber, S. *Phys. Status Solidi* **1997**, A162, 95. (b) Itoh, H.; Ohshima, T.; Aoki, Y.; Abe, K.; Yoshikawa, M.; Nashiyama, I.; Okumura, H.; Yoshida, S.; Uedono, A.; Tanigawa, S. *J. Appl. Phys.* **1997**, 82, 5339.

(21) (a) Wagner, G. W.; Na, B. K.; Vannice, M. A. *J. Phys. Chem.* **1989**, 93, 5061. (b) Apperley, D. C.; Harris, R. K.; Marshall, G. L.; Thompson, D. P. *J. Am. Ceram. Soc.* **1991**, 74, 777.

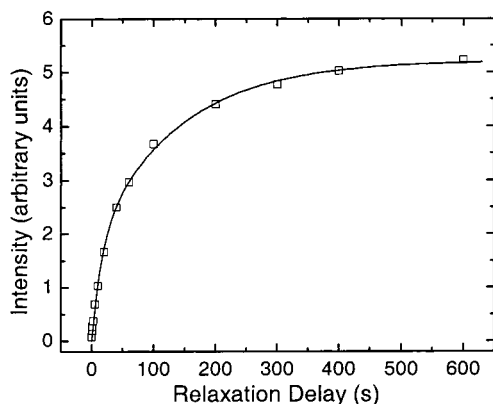


Figure 6. Plot of MAS NMR signal intensity at -18.5 ppm vs saturation-recovery delay time τ for ^{29}Si peaks of as-synthesized silicon carbide powder. The curve was obtained from a four parameter least-squares fit.

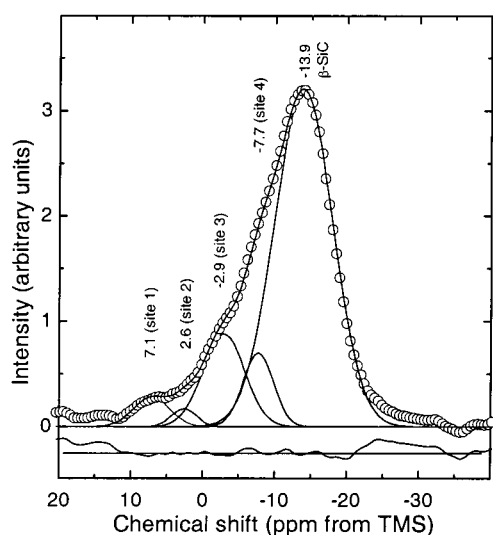


Figure 7. ^{29}Si MAS NMR spectrum of the crushed sample after high-pressure sintering of the as-synthesized powder at 4 GPa and 1800 °C. The curves show a fit using five Gaussian peaks in keeping with the model in Table 1.

plitudes). The four parameter least-squares fit gives relaxation times $T_1^{\text{SiC}} = 137 \pm 20$ s and $T_1^{\text{SiC-C}} = 16 \pm 3$ s. The first value is in good agreement with the relaxation time of ~ 130 s reported for β -SiC.²² Thus, both the relaxation time and the ^{29}Si chemical shift confirm that one of silicon sites in the as-synthesized compound corresponds closely to cubic silicon carbide. The Si sites in the SiC-C region relax ~ 8 times more quickly than those in the cubic domains.

The ^{29}Si NMR spectra of the annealed SiC-C powders show that the downfield shoulder gradually disappears as the temperature increases (Figure 5) and the spectrum of the sample annealed at 1900 °C is virtually identical to that of a standard β -SiC powder. A similar behavior was observed in the diffraction patterns of these samples (Figure 3) as the split peaks transformed to a single diffraction profile of normal β -SiC.

The XRD analysis of the sample sintered at high pressure and a temperature of 1400 °C revealed only the growth of the dislocation density, and it was

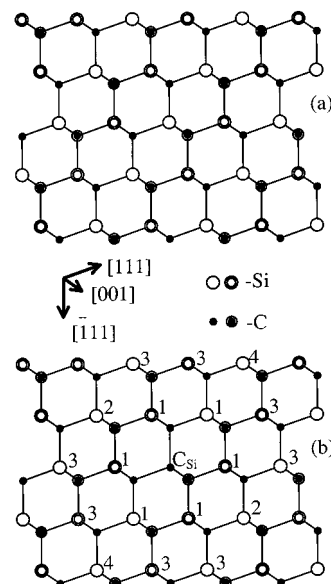


Figure 8. Fragments of the perfect β -SiC (a) and ideal solid solution $\text{Si}_{1-x}\text{C}_{1+x}$ (b) crystal structures [projection onto (110)]. The numeric ticks show the different types of silicon sites (Table 1) formed by C_{Si} in the silicon carbide crystal structure. Open-circle Si and the large-circle C atoms lie out of the plane of the figure.

concluded⁵ that there was no change in the composition and the distribution of the superstoichiometric carbon atoms within the silicon carbide crystallites. This conclusion is supported by the ^{29}Si MAS NMR results. The fine structures of the ^{29}Si NMR peaks of the as-synthesized powder and samples sintered at 1400 °C are similar, and the ratio between the broad (downfield shoulder) and sharp components does not change. XRD analysis of samples sintered at a higher temperature of 1800 °C (see above) shows that redistribution of the excess carbon atoms leads to the formation of an ideal solid solution $\text{Si}_{1-x}\text{C}_{1+x}$. Significant changes are observed in the ^{29}Si NMR spectra when compared to the as-synthesized powder (Figure 7). There is a sharp peak at ca. -14 ppm with downfield peaks. This suggests that the presence of homogeneously distributed superstoichiometric carbon atoms (as carbon antisites C_{Si}) displaces the ^{29}Si MAS NMR signal to lower field and the C_{Si} point defects change the local environment of the neighboring silicon atoms (Figure 8).

The inclusion of carbon antisite point defects up to the fourth neighbor Si shell at 6.17 Å gives rise to four nonstandard Si environments, as listed in Table 1, which can be used to assign the shoulder peaks in Figure 7. The closer the carbon antisite to the silicon atom, the greater the downfield chemical shift in the ^{29}Si NMR spectrum. The intense peak at -14 ppm corresponds to a bulk β -SiC silicon site, but even this is shifted from the normal value of -18 ppm showing that the small excess C content affects the electronic environment in the bulk structure. Attempts to fit the ^{29}Si MAS NMR spectrum with five peaks resulted in several solutions depending on the initial parameters of the least-squares refinement. The fit presented in Figure 7 has a good agreement between the intensity of the fitted peaks and the ratio of proposed types of silicon sites in Table 1 although this is not a uniquely good fit. In all fits, the fraction of the nonstandard silicon sites was in

(22) (a) Inkrott, K. I.; Wharry, S. M.; O'Donnell, D. J. *Mater. Res. Soc. Symp. Proc.* **1986**, 73, 165. (b) Harrison, S.; Xie, X. Q.; Jakubenas, K. J.; Marcus, H. L. *J. Am. Ceram. Soc.* **1999**, 82, 3221.

Table 1. Different Types of Silicon Environments Created by a Carbon Antisite Defect up to the Fourth Si Neighbor Shell in the Cubic Silicon Carbide Crystal Structure; the Values of the Interatomic Distances Correspond to Ideal β -SiC; Data for a Si Site in Standard β -SiC Are Presented for Comparison; the Chemical Shifts Are from the Fit in Figure 7

distance to central Si (Å)	neighbors				β -SiC site
	site 1	site 2	site 3	site 4	
1.89	4C	4C	4C	4C	4C
3.08	11Si, 1C	12Si	12Si	12Si	12Si
3.61	12C	12C	12C	12C	12C
4.36	6Si	5Si, 1C	6Si	6Si	6Si
4.75	12C	12C	12C	12C	12C
5.34	24Si	24Si	23Si, 1C	24Si	24Si
5.66	16C	16C	16C	16C	16C
6.17	12Si	12Si	12Si	11Si, 1C	12Si
multiplicity	12	6	24	12	
chem shifts (ppm)	7.1	2.6	-2.9	-7.7	-13.9

the range of 25–35%. This is consistent with the measurable influence of the carbon antisite defects reaching as far as the fourth neighbor shell of Si (Table 1, Figure 8) which, for an ideal $\text{Si}_{1-x}\text{C}_{1+x}$ solid solution with $x = 0.007$, displaces 32% of the Si signal downfield of the main peak.

Conclusions

XRD and MAS NMR experiments show that two distinct phases of silicon carbide (cubic β -SiC and a SiC–C solid solution) are formed in the self-propagating high-temperature reaction of a mixture of elemental silicon and thermally exfoliated graphite. The structures

of the as-synthesized silicon carbide and samples annealed at 1400–1900 °C in a vacuum or sintered at 4–8 GPa and 1400 or 1800 °C are all consistent with the description of the initial microstructure as SiC–C domains containing a high concentration of the superstoichiometric carbon atoms in diamond-like carbon layers, coexisting with regions of normal β -SiC. Good agreement between the results of XRD and MAS NMR experiments is found for all of the investigated samples.

The breakdown of the domain structure of the crystallites by thermal diffusion during sintering at 4–8 GPa and 1800 °C leads to a homogeneous redistribution of the superstoichiometric carbon atoms as C antisite defects throughout the cubic SiC structure which influence the local and bulk silicon atoms. The $\sim 0.7\%$ excess of carbon in the cubic SiC phase leads to a 4 ppm downfield shift of the bulk ^{29}Si MAS NMR peak, and distinct NMR resonances from sites up to four Si shells away from the carbon antisite defects are also observed. These results confirm a high sensitivity of the silicon chemical shift to slight changes of local environment which is very valuable for studying defects in the various phases of SiC.

Acknowledgment. We thank Dr. J. M. Rawson for collection and discussion of EPR spectroscopy measurements and Dr. M. J. Duer for helpful discussions about the NMR spectroscopy. O.O.M. is grateful to the Royal Society, NATO, and FCO Chevening for a Postdoctoral Fellowship award.

CM011246L